1-1-2007

Computing Boundary Slopes of 2-Bridge Links

Jim Hoste
Pitzer College

Patrick Shanahan
Loyola Marymount University, pshanaha@lmu.edu

MATHEMATICS OF COMPUTATION
Volume 76, Number 259, July 2007, Pages 1521–1545
S 0025-5718(07)01936-9
Article electronically published on March 12, 2007

COMPUTING BOUNDARY SLOPES OF 2-BRIDGE LINKS

JIM HOSTE AND PATRICK D. SHANAHAN

Abstract. We describe an algorithm for computing boundary slopes of 2-bridge links. As an example, we work out the slopes of the links obtained by $1/k$ surgery on one component of the Borromean rings. A table of all boundary slopes of all 2-bridge links with 10 or less crossings is also included.

1. Introduction

In a series of papers by Hatcher and Thurston [7], Floyd and Hatcher [4], and Hatcher and Oertel [6], the set of incompressible, boundary incompressible surfaces in the complement of a 2-bridge knot or link, or a Montesinos knot, are completely described and classified. In the case of knots, these papers also describe the possible boundary slopes that occur, and in [6] a table of all boundary slopes of Montesinos knots with 10 or fewer crossings is given. Unfortunately, this table contains several errors. However a corrected table has been published by Dunfield [3]. Moreover, the computer program written and used by Dunfield is available at `http://www.CompuTop.org`.

While Floyd and Hatcher explicitly describe all incompressible surfaces in the complement of a 2-bridge link, they do not compute the boundary slopes of these surfaces, saying only that it should be possible in principle. In his Ph.D. thesis [9], Lash starts with their construction and shows how to compute the associated boundary slopes. His ultimate goal was to compare the set of boundary slopes of the Whitehead link, $\mathcal{L}_{3/8}$, to those predicted by the algebraic-geometric machinery of Culler-Shalen [2]. Applying his algorithm to $\mathcal{L}_{3/8}$, Lash was able to show that in this case, every boundary slope arises from a degenerating sequence of representations of the link group into $\mathrm{SL}_2\mathbb{C}$. Ohtsuki [10] has shown this to be true for all 2-bridge knots (excluding slopes that correspond to a fiber in a fibration), but the question remains open for all 2-bridge links in general. To investigate this question it would obviously be helpful to have boundary slope data for all 2-bridge links. Unfortunately, Lash's thesis has never been published and tables of boundary slopes of links have not been available.

In this paper we describe Lash's algorithm and develop an improved algorithm. The new algorithm eliminates several computationally intensive steps. With a little practice it can be readily applied by hand, and is easier to implement on a computer. This allows us to describe the types of boundary slopes that can occur. As an illustration of our techniques, we compute the boundary slopes of

Received by the editor May 24, 2005 and, in revised form, March 31, 2006.
2000 *Mathematics Subject Classification.* Primary 57M25.
Key words and phrases. Knot, link, 2-bridge, boundary slope.

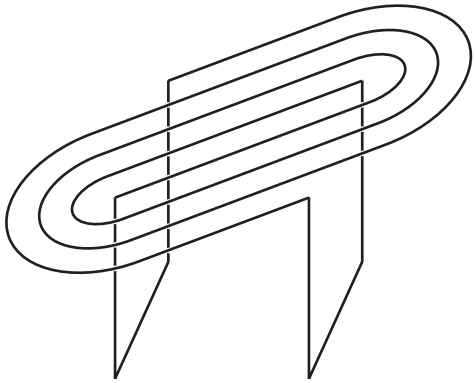

FIGURE 1. The 2-bridge link $\mathcal{L}_{p/q}$, for $p = 3$ and $q = 4$.

the $(4k-1)/(8k)$ 2-bridge links. These links may also be described as $1/k$ surgery on one component of the Borromean rings. For this class of links, we have found an explicit description of their eigenvalue varieties and in a forthcoming paper will investigate the relationship between the actual boundary slopes and those detected by the eigenvalue variety.

We have written a computer program to implement our algorithm and include here a table of boundary slopes of all 2-bridge links up to 10 crossings. In our table, links through 9 crossings are also identified by their index in Rolfsen's table [11]. Our program, as well as a much larger table to 16 crossings, will eventually be available at `http://www.CompuTop.org` and as part of *Knotscape* [8].

In Section 2 we briefly describe Floyd and Hatcher's construction for 2-bridge links. The reader is referred to their original paper for more detail. Then in Section 3 we describe Lash's algorithm for finding the boundary slopes of a given 2-bridge link using Floyd and Hatcher's construction. In Section 4 we improve the algorithm and discuss some of its theoretical consequences. The next section includes a nice example for the infinite family of 2-bridge links already mentioned above. Finally, in Section 6 we tabulate boundary slope data for all 2-bridge links with 10 or less crossings.

2. Floyd and Hatcher's construction

Let p and q be relatively prime positive integers such that $0 < p < q$, p is odd, and q is even. We assume that the reader is familiar with the standard 2-bridge diagram of the 2-bridge link $\mathcal{L}_{p/q}$. For example, $\mathcal{L}_{3/4}$ is shown in Figure 1. It is important to note that our definition of $\mathcal{L}_{p/q}$ agrees with that of [6] and [9], but is the mirror image of the more conventional depiction of $\mathcal{L}_{p/q}$ with the "(straight) bridges on top." See for example, [1] or [7].

Viewing S^3 as the 2-point compactification of $S^2 \times \mathbb{R}$, we may place $\mathcal{L}_{p/q}$ in $S^2 \times I$ so that it meets $S^2 \times \{0\}$ and $S^2 \times \{1\}$ each in two arcs, and each intermediate level in four points. We may think of each level, $S^2 \times \{z\}$, as the quotient $\mathbb{R}^2/\Gamma$, where Γ is the group generated by 180° rotations of $\mathbb{R}^2$ about the integer lattice points $\mathbb{Z}^2$. The four points of the link at each intermediate level are precisely the four points of $\mathbb{Z}^2/\Gamma$. The arcs at level $z = 1$ are the image of the lines in $\mathbb{R}^2$ which pass through integer lattice points with slope p/q. Similarly, the two arcs at level

$z = 0$ are the image of vertical lines through integer lattice points. Finally, $\mathrm{PSL}_2\mathbb{Z}$ acts linearly on each level, leaving $\mathbb{Z}^2/\Gamma$ invariant.

Floyd and Hatcher next describe four basic branched surfaces, $\Sigma_A, \Sigma_B, \Sigma_C$ and Σ_D, copies of which will be stacked, one on top of the other, to build a branched surface spanning the 2-bridge link. Actually it is not these surfaces exactly, but rather homeomorphic images of them, that will be compressed vertically and stacked together. To understand the Floyd and Hatcher construction, and Lash's computation of the boundary slopes, we need to first understand these four basic building blocks.

Beautiful illustrations of the four surfaces are given in [4] which we will not attempt to reproduce here. Instead, we describe the surfaces in a different fashion. Each is contained in $S^2 \times I$. In both of the half-intervals $[0, \frac{1}{2})$ and $(\frac{1}{2}, 1]$ the surface is a product of the half-interval with a finite number of disjoint embedded arcs in the 2-sphere with endpoints at the four points of $\mathbb{Z}^2/\Gamma$. The transversality of the surface with the horizontal levels completely degenerates at the $\frac{1}{2}$-level, where branching occurs which allows the arc system at the 0-level to transition to the arc system at the 1-level. Figure 2 shows cross-sections of each branched surface at heights $0, \frac{1}{2}$, and 1. At the $\frac{1}{2}$-level the shaded areas indicate horizontal parts of the surface. Each of the four branched surfaces can carry a variety of embedded surfaces in the usual way indicated by the number of sheets, or weights, on each piece of the branched surface. The weights are also indicated in Figure 2 as well as arrows at the $\frac{1}{2}$-level which indicate the direction of branching as one moves up from the 0-level to the 1-level. Finally, notice that all the surfaces shown in Figure 2 carry the implicit assumption that $\alpha > \beta$ (and sometimes that α and β have the same parity).

If $g = \begin{pmatrix} a & b \\ c & d \end{pmatrix}$ is any element of $\mathrm{PSL}_2\mathbb{Z}$, let $\hat{g} = \begin{pmatrix} d & c \\ b & a \end{pmatrix}$. We may take $S^2 \times I$ to itself with the homeomorphism $\hat{g}\times\mathrm{id}$ and carry any one of the four basic surfaces to a new branched surface that begins and ends at arc systems with slopes depending on g. Images like this of the four basic surfaces can then be joined together vertically provided they have matching arc systems where they are attached. In this way we can piece together a branched surface that begins with the two arcs of $\mathcal{L}_{p/q}$ at level 0 of slope $\frac{1}{0}$ and ends with the two arcs of $\mathcal{L}_{p/q}$ at level 1 of slope $\frac{p}{q}$. For example, suppose we begin with the Hopf link, $\mathcal{L}_{1/2}$. We wish to piece together a branched surface that starts at slope $\frac{1}{0}$ and ends at slope $\frac{1}{2}$. Starting with a copy of Σ_A we may move from two arcs at slope $\frac{1}{0}$ to an arc system consisting of three arcs: one at slope $\frac{1}{0}$ and two at slope $\frac{0}{1}$. We may then attach to this an upside-down copy of Σ_D which then takes us to an arc system of three arcs: two at slope $\frac{0}{1}$ and one at slope $\frac{1}{2}$. Finally, we will end with an upside-down copy of Σ_A transformed by $\hat{g}\times\mathrm{id}$ where $g = \begin{pmatrix} 1 & 0 \\ 2 & 1 \end{pmatrix}$. Notice that the linear transformation $\hat{g}$ takes lines of slope $\frac{1}{0}$ to lines of slope $\frac{1}{2}$ and lines of slope $\frac{0}{1}$ to lines of slope $\frac{0}{1}$, because

$$\begin{pmatrix} 1 & 2 \\ 0 & 1 \end{pmatrix}\begin{pmatrix} 0 \\ 1 \end{pmatrix} = \begin{pmatrix} 2 \\ 1 \end{pmatrix} \quad \text{and} \quad \begin{pmatrix} 1 & 2 \\ 0 & 1 \end{pmatrix}\begin{pmatrix} 1 \\ 0 \end{pmatrix} = \begin{pmatrix} 1 \\ 0 \end{pmatrix}.$$

Therefore, the upside-down copy of Σ_A transformed by $\hat{g}\times\mathrm{id}$ ends with the desired arc system of two arcs of slope $\frac{1}{2}$.

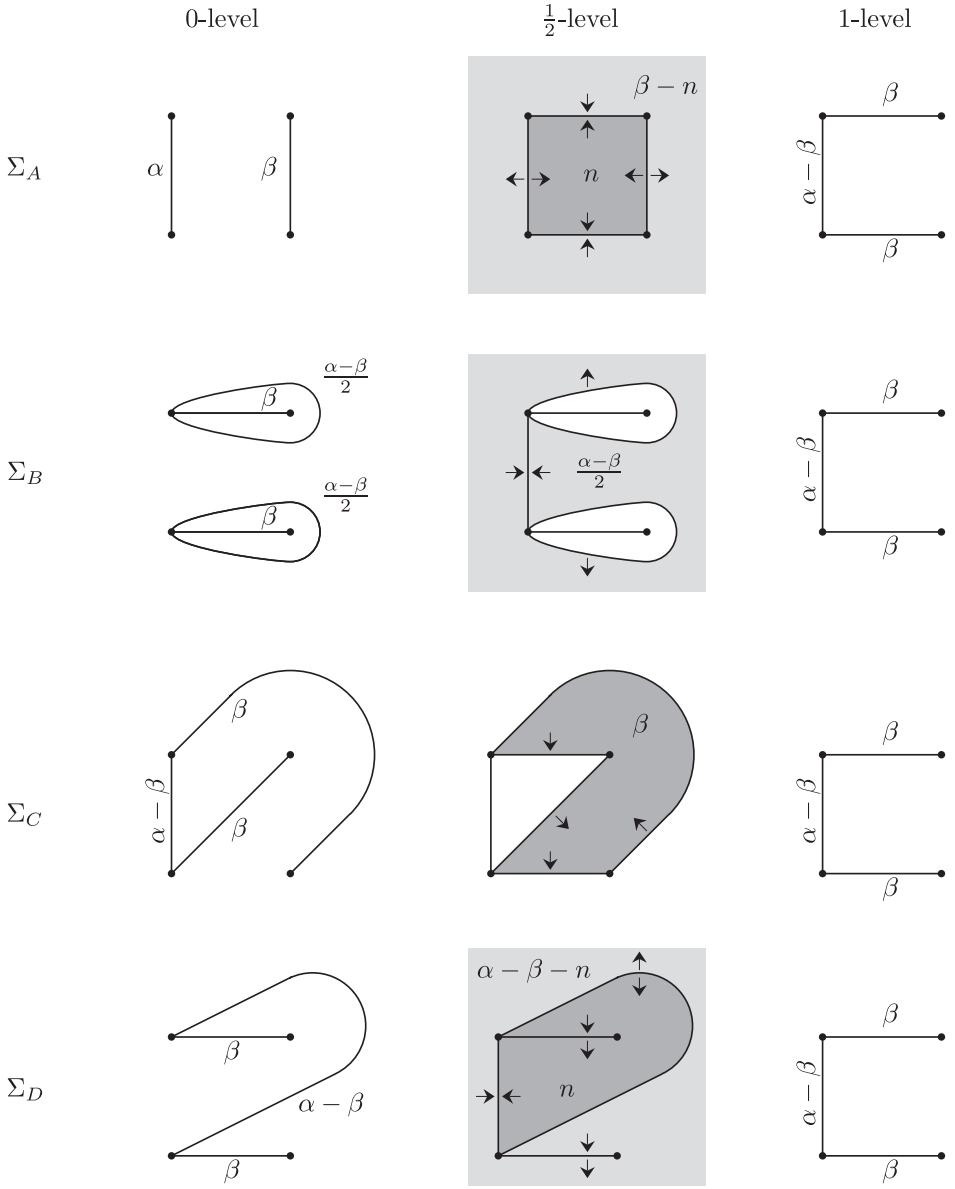

FIGURE 2. The four basic branched surfaces.

There is a beautiful correspondence between branched surfaces constructed in this way and continued fraction expansions of p/q which in turn may be viewed as paths in the following diagrams. Consider first the tessellation D_1 of $\mathbb{H}^2$ by ideal triangles shown in Figure 3. The rationals, together with $\frac{1}{0}$, are arranged around the unit circle as shown, and two fractions $\frac{a}{b}$ and $\frac{c}{d}$ are connected by a geodesic if and only if $ad - bc = \pm 1$. (This diagram contains the Stern-Brocot tree generated from $\frac{1}{0}$ and $\frac{0}{1}$ by adding fractions the "wrong way" according to the (mis)rule $\frac{a}{b} + \frac{c}{d} = \frac{a+c}{c+d}$. See [5], for example.) The group of orientation preserving symmetries

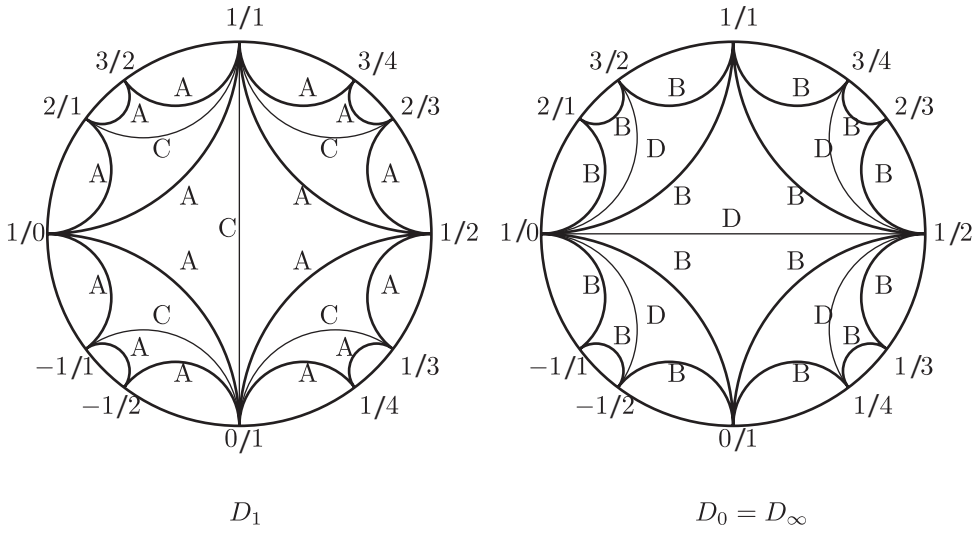

FIGURE 3. The diagrams D_0, D_1, and D_∞.

of D_1 is $\mathrm{PSL}_2\mathbb{Z}$. Let $G \subset \mathrm{PSL}_2\mathbb{Z}$ be the subgroup of Möbius transformations given by $z \to \frac{az+b}{cz+d}$ where c is even. It follows that the triangle $\{\frac{1}{0}, \frac{0}{1}, \frac{1}{1}\}$ is a fundamental domain for the action of G and the G-images of the ideal quadrilateral $Q = \{\frac{1}{0}, \frac{0}{1}, \frac{1}{2}, \frac{1}{1}\}$ tessellate $\mathbb{H}^2$. If we delete the G-orbit of the diagonal $\{\frac{0}{1}, \frac{1}{1}\}$ and replace it with the G-orbit of the opposite diagonal $\{\frac{1}{0}, \frac{1}{2}\}$, we obtain a new diagram called D_0, which is also shown in Figure 3.

Between D_0 and D_1 there exists a family of oriented diagrams D_t, for $0 < t < 1$, obtained by expanding each diagonal in D_1 (labeled C in Figure 3) to a rectangle which may then be collapsed to the opposite diagonal (labeled D in Figure 3), thus giving D_0. The intersection of each of D_0, D_t, and D_1 with the fundamental quadrilateral Q is shown in Figure 4. The edges of D_t fall into four G-orbits which are named A, B, C, and D and which have, respectively, representative edges A_0, B_0, C_0 and D_0 as defined in Figure 4. As $t \to 0$ the edges degenerate into B and D-type edges in D_0. If instead, $t \to 1$, the edges degenerate into A and C-type edges in D_1. We may orient the edges of D_t by using the orientations of A_0, B_0, C_0 and D_0 shown in Figure 4, but there is no coherent way to orient the edges of D_0 or D_1. Finally, by setting $D_t = D_{1/t}$ for $1 \le t \le \infty$, we obtain a diagram for every $t \in [0, \infty]$.

Floyd and Hatcher show that the diagram D_t provides a beautiful way of describing all the incompressible surfaces in the 2-bridge link exteriors. In particular, *minimal edge paths* in D_t from $\frac{1}{0}$ to $\frac{p}{q}$ will correspond to branched surfaces which in turn will carry the incompressible surfaces. An edge path in D_t is *minimal* if it never contains two consecutive edges that lie in the same triangle or rectangle of D_t. It is not hard to see that a minimal edge path in D_t (with $t \notin \{0, 1, \infty\}$) will collapse to a minimal edge path in either D_0 or D_1 as t approaches 0 or 1 respectively. Moreover, these limiting paths in D_0 and D_1 uniquely determine the path in D_t. For a particular fraction $\frac{p}{q}$ there can only be a finite number of minimal edge paths connecting it to $\frac{1}{0}$. This follows from the fact that these minimal paths are all contained in a unique minimal chain of quadrilaterals consisting of Q and a finite number of its translates under G.

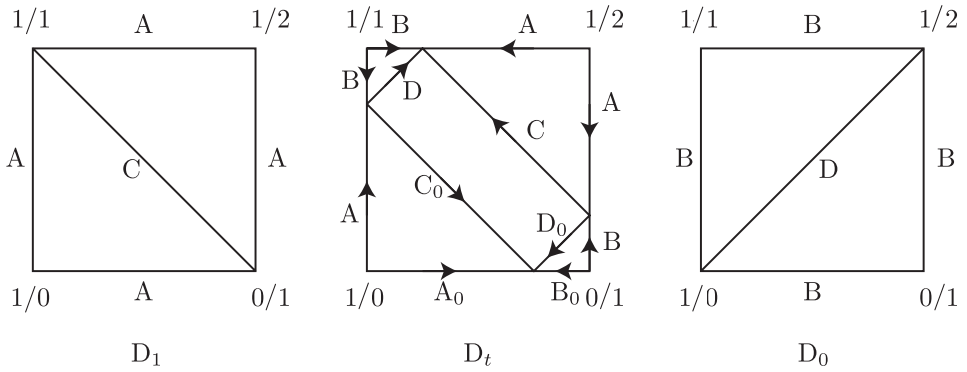

FIGURE 4. Expanding the diagonals of D_0 and D_1 to obtain D_t (pictured here with $t = 3/4$).

Each minimal edge path in D_t (with $t \notin \{0, 1, \infty\}$) from $\frac{1}{0}$ to $\frac{p}{q}$ provides a recipe for piecing together images of the four basic surfaces $\Sigma_A, \Sigma_B, \Sigma_C$, and Σ_D as follows. Suppose γ is a path consisting of consecutive edges $e_1, e_2, \ldots, e_m$. For each edge e_i there exists an element $g_i \in G$ taking E_i to e_i, where E_i is one of the four representative edges A_0, B_0, C_0, or D_0 in Q. Let S_i be $\Sigma_A, \Sigma_B, \Sigma_C$, or Σ_D depending on whether E_i is A_0, B_0, C_0, or D_0 respectively. Now take S_i to $(\hat{g}_i \times \mathrm{id})(S_i)$, rescaling vertically so as to place the image in $S^2 \times [\frac{i-1}{m}, \frac{i}{m}]$. Moreover, if the orientation of $g_i(E_i)$ is opposite to that of e_i, we first reflect S_i through the 2-sphere $S^2 \times \{\frac{1}{2}\}$ before applying $\hat{g}_i \times \mathrm{id}$.

If t is rational and equal to the reduced fraction α/β, we can further use this information to assign weights to the branched surface as follows. If $t > 1$ the branched surface is weighted as shown in Figure 2. If instead, $0 < t < 1$, the above construction is altered by first rotating each of the basic surfaces $\Sigma_A, \Sigma_B, \Sigma_C$, and Σ_D through 180° in the obvious way so as to interchange the two components of $\mathcal{L}_{p/q}$. We then swap α and β and proceed as before. Thus for every minimal edge path in D_t with t a positive rational number different from 1, we have associated a weighted branched surface and thus an actual surface in the complement of the link.

If $t = 0, 1$, or ∞ we must modify this recipe slightly. If we let t approach zero or infinity, then the above constructions will limit at surfaces for which $\alpha = 0$ or $\beta = 0$ respectively. But the limiting surfaces which arise from the above constructions when $\alpha \to \beta$ do not give all desired surfaces with $\alpha = \beta$. Instead, the process must be modified slightly. As $t \to 1$ the minimal edge paths in D_t approach minimal edge paths in D_1 that consist entirely of A or C-type edges. Returning to Figure 2, notice that if $\alpha - \beta = 0$, then Σ_A with $n = \alpha$ and Σ_C are isotopic. Thus if C-type edges are involved, then Σ_A allows for more general branching than Σ_C, and for this reason we replace each use of Σ_C with Σ_A.

Finally, the main result of Floyd and Hatcher is the following theorem.

Theorem 2.1 (Floyd and Hatcher)**.** *The orientable incompressible and meridionally incompressible surfaces in $S^3 - \mathcal{L}_{p/q}$, without peripheral components, are exactly (up to isotopy) the orientable surfaces carried by the collection of branched surfaces associated to minimal edge paths in D_t from $\frac{1}{0}$ to $\frac{p}{q}$ and with $t \in [0, \infty]$.*

Recall from [4] that a surface S in the complement of the link L is *meridionally incompressible* if whenever there is a disk $D \subset S^3$ with $D \cap S = \partial D$ and such that D meets L transversely in one interior point, then there exists a disk $D' \subset S \cup L$ with $\partial D = \partial D'$ and such that D' also meets L transversely in a single interior point.

Floyd and Hatcher then go on to explicitly describe when two surfaces constructed in this way are isotopic. However, they do not compute the boundary slopes of these surfaces, saying only that it should be possible in principle.

3. Lash's algorithm

The boundary of a branched surface derived from the Floyd-Hatcher construction defines a train track on the boundary of the regular neighborhood of the link. Thus the boundary of any incompressible surface carried by the branched surface is carried by this train track. Lash's first step is to determine the train tracks for each of the four basic surfaces $\Sigma_A, \Sigma_B, \Sigma_C$ and Σ_D.

Before doing this, we introduce some notation. Let the four points of $\mathbb{Z}^2/\Gamma$ be $(0,0), (1,0), (0,1)$ and $(1,1)$. At the 0-level, assume that the two arcs of $\mathcal{L}_{p/q}$ join the points $(0,0)$ to $(0,1)$ and $(1,0)$ to $(1,1)$. Furthermore, let $\mathcal{L}_{p/q} = \{K_1, K_2\}$ where K_1 contains $(0,0)$ and $(0,1)$. Orient K_1 so that it runs vertically upward from $(0,0)$ and orient K_2 so that it runs vertically upward from $(1,1)$. Choose as a fundamental domain of $\mathbb{R}^2/\Gamma$ the region $\mathcal{D} = [0,1] \times [-1/2, 3/2]$. Removing small disks of radius ϵ centered at the four points of $\mathbb{Z}/\Gamma$ will remove semi-disks from the fundamental domain $\mathcal{D}$. These correspond to meridional cross sections of the regular neighborhood of the link.

Let μ_1 be the oriented meridian of K_1 having linking number $+1$ with K_1. Let λ_1 be the oriented longitude of K_1 defined as follows. Start with the line segment from $(0, 1-\epsilon, \epsilon)$ to $(0, \epsilon, \epsilon)$. Join to this the vertical segments $\{(0,\epsilon)\} \times [\epsilon, 1-\epsilon]$ and $\{(0, 1-\epsilon)\} \times [\epsilon, 1-\epsilon]$. Next, add the curve in $\mathbb{R}^2 \times \{1-\epsilon\}$ which starts at $(0, \epsilon, 1-\epsilon)$, ends at $(0, 1-\epsilon, 1-\epsilon)$, and is parallel to K_1. Finally, orient λ_1 parallel to K_1.

The 180° rotation of Figure 1 about the vertical axis $\{(1/2, 1/2)\} \times \mathbb{R}$ interchanges the components of the link, and preserves their orientations. We define the oriented meridian μ_2 and longitude λ_2 of K_2 as the images of μ_1 and λ_1 respectively under this rotation.

We will initially compute all boundary slopes with respect to the basis $\{\mu_i, \lambda_i\}$. However, λ_i is not necessarily a preferred longitude of K_i, so it will be necessary later to know its linking number with K_i. It is a straightforward exercise to compute this. We obtain

$$\mathrm{lk}(K_i, \lambda_i) = -\sum_{j=1}^{\frac{q-2}{2}} (-1)^{[\![2jp/q]\!]} \tag{3.1}$$

where $[\![x]\!]$ is the greatest integer less than or equal to x. Note, for example, that λ_i is never the preferred longitude if q is a multiple of 4 since the linking number must be odd in this case.

Figure 5 depicts the train track boundaries of each of the four basic branched surfaces. Each row of the figure shows the train tracks on the boundary of each of

the four "columns" which are the regular neighborhoods of the vertical segments of the link. These are depicted in the corresponding regions of $\mathcal{D} \times [0,1]$, that is, the product of the semicircular arcs surrounding each integer lattice point with the unit interval $[0,1]$. Notice that we have used slopes ranging from $-\infty$ to ∞ to parameterize the semicircular arcs. Thus we see the train tracks for Σ_A, on each of the four columns, begin at slopes of $\pm\infty$ and end at slopes of $\pm\infty$ and 0. Similarly, the train tracks for Σ_C, on all four columns, have curves that begin at slopes of 1 and end at slopes of 0.

Suppose Σ is a branched surface obtained by piecing together homeomorphic copies of the four basic branched surfaces and that S is a surface carried by Σ. Because Σ corresponds to a path in D_t from $\frac{1}{0}$ to $\frac{p}{q}$, Σ will always begin with a copy of Σ_A and end with an upside-down copy of Σ_A. Let the initial weights on Σ at the 0-level be α and β as shown in Figure 2. Thus, at the 0-level on the neighborhood of K_1, the boundary of S consists of α arcs. If we orient one of these arcs in the direction of K_1 and follow it upward, it will follow the train track up the $(0,0)$ column until it reaches the top, traverse a curve of slope $\frac{p}{q}$ at the 1-level, and then follow the train track down the $(0,1)$ column. In Figure 5 we have chosen to orient the train tracks parallel to K_1 and K_2 for this reason. When we return to our starting point at the bottom we may end there, or perhaps continue to travel around again in the longitudinal direction. If the boundary of S consists of several components, we may orient them all parallel to K_1 and K_2 (even if these orientations are not compatible with an orientation of S).

Suppose ∂S has k components on the regular neighborhood of K_1 and that each has algebraic (and geometric) intersection of l_i with μ_1. Thus

$$l_1 + l_2 + \cdots + l_k = \alpha.$$

Furthermore, suppose each has algebraic intersection m_i with λ_1. Then $\gcd(m_i, l_i) = 1$ for all i and moreover, because the components of ∂S are all disjoint and nontrivial, each boundary slope m_i/l_i is the same. From this it follows that l_i and m_i are constant, say $l_i = l$ and $m_i = m$. Thus to determine the boundary slope m/l we need only compute the total algebraic intersection $M_1 = m_1 + m_2 + \cdots + m_k$ of ∂S with λ_1 and divide it by α. Similarly, the boundary slope of S on the regular neighborhood of K_2 is M_2/β where M_2 is the total algebraic intersection of ∂S with λ_2. Again, these boundary slopes are with respect to the basis $\{\mu_i, \lambda_i\}$.

To compute M_1 we must sum the algebraic intersection of the oriented train tracks with λ_1 on columns $(0,0)$ and $(0,1)$. We may do this one section at a time, with each section coming from one of the four basic surfaces. We may simplify matters by pulling back λ_1 under the inverse of $\hat{g}\times\mathrm{id}$ and counting its intersection with the standard train tracks shown in Figure 5, rather than examining the images of the standard train tracks under $\hat{g}\times\mathrm{id}$. If $g = \begin{pmatrix} a & b \\ c & d \end{pmatrix}$, then $\hat{g}^{-1} = \begin{pmatrix} a & -c \\ -b & d \end{pmatrix}$ and the vector $\begin{pmatrix} 0 \\ 1 \end{pmatrix}$, which represents a slope of ∞ (and the longitude λ_1), pulls back to the vector $\begin{pmatrix} -c \\ d \end{pmatrix}$, which represents a slope of $-d/c$. Thus we must examine how the standard train tracks intersect the vertical line located at slope $-d/c$.

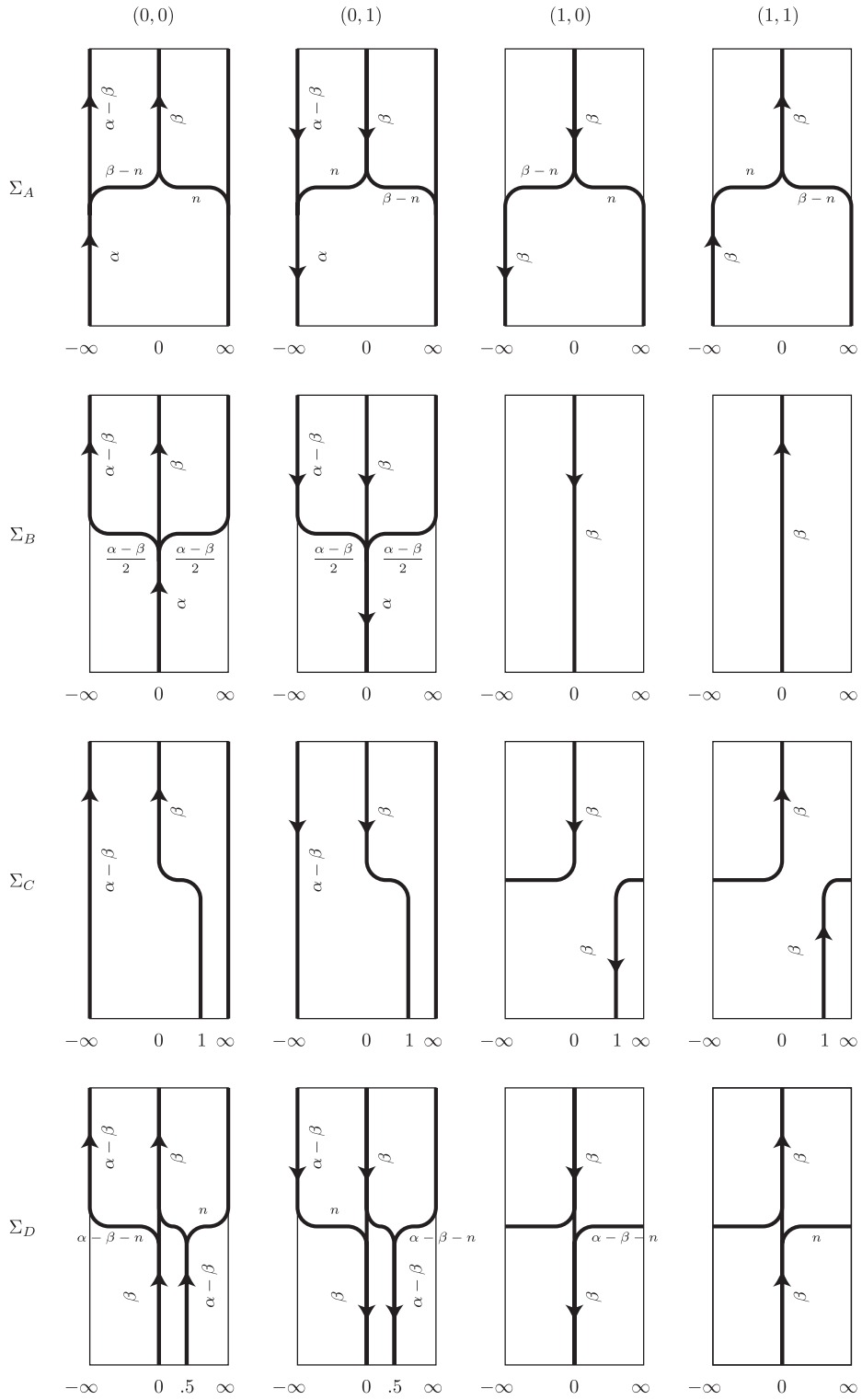

FIGURE 5. Train track boundaries of each of the four branched surfaces.

For example, suppose γ is a minimal edge path in D_t beginning at $\frac{1}{0}$ and ending at $\frac{p}{q}$. Let e_i be an edge of γ that is the image of $E_i = A_0$ under the element g_i of G. Furthermore, suppose that the orientations of e_i and $g_i(A_0)$ agree. If $0 < -d/c < \infty$, then the algebraic intersection on column $(0,0)$ is $-n$ and on column $(0,1)$ is $-(\beta - n)$. Note that on column $(0,0)$ the meridian runs from 0 towards ∞ while on column $(0,1)$ the meridian runs from 0 to $-\infty$. This explains the minus signs in the above calculations. The total contribution to M_1 at this level, in this case, is thus $-\beta$. If instead, $-\infty < -d/c < 0$, we obtain $\beta - n$ on column $(0,0)$ and n on column $(0,1)$ for a total contribution to M_1 of β. Note that $-d/c$ cannot be zero. This is because c is even and therefore both a and d must be odd since $\det(g) = 1$. However, $-d/c$ may equal $\pm\infty$ if $c = 0$. In this case the train track is not transverse to the (pullback of the) longitude. When this occurs, we may isotope the longitude slightly by pushing it in the positive direction of μ_1. So in this case, if $-d/c = \pm\infty$ we obtain an intersection on column $(0,0)$ of $\beta - n$ and on column $(0,1)$ of $-(\beta - n)$ for a net contribution to M_1 of zero. Table 1 lists these results together with the contributions to M_1 for the other three types of surfaces, all in the case where the orientations of e_i and $g_i(E_i)$ agree. If these orientations are opposite, then we must flip each surface upside-down, and it is easy to see that the effect is to negate the entries in the table.

A similar examination of the standard train tracks allows us to compute M_2. However in this case an additional consideration seems necessary. For any $g \in G$, $\hat{g}$ takes $(0,0)$ to itself and $(0,1)$ to itself since c is even and both a and d are odd. But if b is odd, then $(1,0)$ and $(1,1)$ will be traded while if b is even these lattice points will each be fixed. Thus it seems necessary to consider these cases separately. However, a close examination of the case when b is odd reveals that both the orientations of the train tracks as well as the orientation of μ_2 are reversed and the total contribution to M_2 is unaffected. Thus separate formulae for b even or odd are not needed. The results for each of the four basic surfaces are listed in Table 1.

The data in the first four rows of Table 1 are sufficient to compute the boundary slopes when $t = \alpha/\beta \notin \{0, 1, \infty\}$ and even in the limiting cases $t \to 0$ or $t \to \infty$. But as mentioned already, when $t \to 1$, if any C-type edges appear in the limiting minimal path in D_1, then we replace the corresponding C-type surfaces with the more general A-type surfaces. Suppose e is such a C-type edge in D_1. Then e joins a/c and b/d in D_1 where both c and d are odd, $ad - bc = 1$, and thus, exactly one of a or b is even. Therefore we may choose $g = \begin{pmatrix} a & b \\ c & d \end{pmatrix}$ and assume that b is even, while a, c, and d are all odd. Now $\hat{g}$ fixes $(0,0)$ and $(1,0)$ while trading $(0,1)$ and $(1,1)$. To properly use Figure 5 now, we must orient columns $(0,0)$ and $(0,1)$ up and the other two down. Furthermore, the meridian μ_1 points from 0 to ∞ in the $(0,0)$ figure and from 0 to $-\infty$ in the $(1,1)$ figure. Similarly, the meridian μ_2 points from 0 to ∞ in the $(0,1)$ figure and oppositely in the $(1,0)$ figure. It is now a simple matter to compute the contributions to M_1 and M_2 given in the last row of Table 1. Here we see that the number n of horizontal sheets does not cancel from the calculations. Notice also that because both c and d are odd, $-d/c$ cannot equal zero or infinity.

Everything is now in place to compute the boundary slopes for a given 2-bridge link, $\mathcal{L}_{p/q}$. Beginning with $0 < \beta < \alpha$, and hence $1 < t < \infty$, we first find all

TABLE 1. Contributions to M_1 and M_2 according to surface type.

Surface Type	M_1	M_2	$-d/c$
A	β	β	$-\infty < -d/c < 0$
	$-\beta$	$-\beta$	$0 < -d/c < \infty$
	0	0	$-d/c = \pm\infty$
B	$\beta - \alpha$	0	$-\infty < -d/c < 0$
	$\alpha - \beta$	0	$0 < -d/c < \infty$
	0	0	$-d/c = \pm\infty$
C	-2β	0	$0 < -d/c < 1$
	0	2β	otherwise
D	$\beta - \alpha$	$\alpha - \beta$	$-\infty < -d/c < 1/2$
	0	$\alpha - \beta$	$-d/c = 1/2, \pm\infty$
	$\alpha - \beta$	$\alpha - \beta$	$1/2 < -d/c < \infty$
A for C	$2(\beta - n)$	$2n$	$-\infty < -d/c < 0$
	$-2n$	$2(n - \beta)$	$0 < -d/c < \infty$

minimal paths in D_t from $1/0$ to p/q. For each of these paths, each edge e must be identified as the image of $E \in \{A_0, B_0, C_0, D_0\}$ by some element $g = \begin{pmatrix} a & b \\ c & d \end{pmatrix} \in G$. Next, using $-d/c$ and the data in Table 1, the contributions to M_1 and M_2 are computed, and these are added over all edges in the path to obtain M_1 and M_2. Note that the entries in the table must be negated if the orientation of e does not match that of $g(E)$. Notice also that M_1 and M_2 are always integer linear combinations of α and β. The boundary slope of this surface is then

$$\frac{M_1}{\alpha} = \frac{x\alpha + y\beta}{\alpha} = x + yt^{-1}$$

on the boundary associated to K_1 and

$$\frac{M_2}{\beta} = \frac{z\alpha + w\beta}{\beta} = zt + w$$

on the boundary associated to K_2. This gives a 1-parameter family of boundary slopes for each rational number t greater than 1. As t approaches ∞ we may simply take the limits of the slopes obtained so far provided $z \neq 0$. In this case the limiting boundary slopes are x and ∞. However, care should be taken in interpreting the limiting 4-tuple, $(M_1(\alpha, \beta), \alpha, M_2(\alpha, \beta), \beta) \to (x\alpha, \alpha, z\alpha, 0)$. The orientations of K_1 and K_2 give well-defined intersection numbers for curves which intersect a meridian. For curves which are parallel to a meridian, we have not distinguished between whether they agree or disagree with the meridian's orientation. Therefore, the limiting 4-tuples $(x\alpha, \alpha, z\alpha, 0)$ and $(x\alpha, \alpha, -z\alpha, 0)$ correspond to the same surface. If $z = 0$, then M_2 and β both approach zero as t approaches ∞. This means that the surface has no intersection with the regular neighborhood of K_2 and thus has no boundary slope associated with K_2. It should be noted that we have not sought to impose the "meridional incompressibility" condition described in [4] on these limiting surfaces. At the other extreme, letting t approach 1 will

produce legitimate boundary slopes, but not all possible slopes with $\alpha = \beta$. Instead we must consider the limiting minimal edge path in D_1, swap A for C-type edges (if there are any) and now use the data from the last row of Table 1. Finally, to allow for $t < 1$, we must rotate all our surfaces 180° around the axis $\{(1/2, 1/2)\} \times \mathbb{R}$, thus trading α with β. The 4-tuple $(M_1(\alpha,\beta), \alpha, M_2(\alpha,\beta), \beta)$ of the algebraic intersections with $\lambda_1, \mu_1, \lambda_2$, and μ_2 respectively is then transformed to $(M_2(\beta,\alpha), \alpha, M_1(\beta,\alpha), \beta)$ with it now the case that $\alpha < \beta$. Letting t approach zero now corresponds to letting α approach zero. As with the case $t \to \infty$, if the boundary curves on component one are meridians, then there is an ambiguity of sign in the first entry of the 4-tuple. Furthermore, some surfaces with $\alpha = 0$ may be meridionally compressible. Finally, all of these computations are with respect to the bases $\{\mu_1, \lambda_1\}$ and $\{\mu_2, \lambda_2\}$. To convert to a preferred basis, we must consider the linking number $l = \text{lk}(\lambda_1, K_1) = \text{lk}(\lambda_2, K_2)$ given in Equation (3.1). Converting to the preferred basis sends the 4-tuple $(M_1, \alpha, M_2, \beta)$ to $(M_1 + l\alpha, \alpha, M_2 + l\beta, \beta)$.

4. An improved algorithm

As mentioned already, M_1 and M_2 are always integer linear combinations of α and β. After implementing Lash's algorithm on a computer and looking at sample data, the conclusions of the following theorem were apparent. In searching for a proof, we were led to a revision of Lash's algorithm that is much simpler to apply by hand and implement on a computer. The revised approach will be described in the proof and illustrated in the next section with an interesting example.

Before stating some results we define $M(\gamma)$ to be the pair of intersection numbers (M_1, M_2) associated to the path γ in D_t.

Theorem 4.1. *Given any path γ (not necessarily minimal) in D_t with $1 < t < \infty$, which begins and ends at vertices of D_1, $M(\gamma)$ is of the form*

$$M(\gamma) = (x\alpha + y\beta, y\alpha + z\beta)$$

where $x \equiv z \mod 2$. If additionally, γ begins at $\frac{1}{0}$ and ends at $\frac{p}{q}$, then $x + y \equiv 1 + q \mod 2$.

The proof of this theorem is an easy consequence of the following two lemmas.

Lemma 4.2. *Suppose γ_t is a path in D_t starting at $\frac{p_0}{q_0}$, ending at $\frac{p_n}{q_n}$ and consisting solely of A and B-type edges. Letting $t \to 1$, γ_t will collapse to the path*

$$\gamma_1 = \left\{ \frac{p_0}{q_0}, \frac{p_1}{q_1}, \ldots, \frac{p_n}{q_n} \right\}$$

in D_1 containing only A-type edges. Then

$$M(\gamma_t) = \left(\sum_{i=0}^{n-1} \delta_i \right) (\alpha, \beta) \text{ and}$$

$$M(\gamma_1) = \left(\sum_{i=0}^{n-1} \delta_i \right) (\beta, \beta)$$

where

$$\delta_i = \begin{cases} 0, & \text{if } q_i q_{i+1} = 0; \\ p_i q_{i+1} - p_{i+1} q_i, & \text{otherwise.} \end{cases}$$

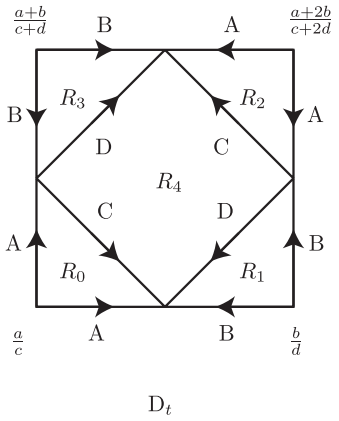

FIGURE 6. Lemma 4.3 describes the result of traveling around each region.

Proof. Let e be an edge of γ_1 oriented from $\frac{a}{c}$ to $\frac{b}{d}$ where a, b, c and d are all positive, c is even and $ad-bc = \pm 1$. The corresponding matrix $g \in G$ is either $g = \begin{pmatrix} a & b \\ c & d \end{pmatrix}$ or $g = \begin{pmatrix} a & -b \\ c & -d \end{pmatrix}$, whichever one has determinant one. In γ_t, e begins with an A-type edge, oriented forward, and ends with a B-type edge, oriented backwards. Referring to Table 1, we see that the contribution to (M_1, M_2) is either $(0,0)$ if $c = 0$, or $(ad-bc)(\alpha, \beta)$. It is easy to check the remaining case where c is odd and d is even. □

Lemma 4.3. *Let $g = \begin{pmatrix} a & b \\ c & d \end{pmatrix}$ be any element of G and label the regions of $g(Q)$ as shown in Figure 6. If $\gamma_i = \partial R_i$, oriented counterclockwise, then $M(\gamma_i)$ are given by:*

γ_i	$M(\gamma_i)$
γ_0 *or* γ_2	$(0, -2\beta)$
γ_1 *or* γ_3	$(-\alpha+\beta, \alpha-\beta)$
γ_4	$(-2\beta, -2\alpha+4\beta)$

Proof. Suppose $g = \begin{pmatrix} a & b \\ c & d \end{pmatrix}$ and consider the path γ_0. The first edge in the path is of type A and is oriented forward, the second is type C oriented backwards, and the final edge is type A oriented backwards. The matrix g is used to determine the contribution of the first two edges, while $\begin{pmatrix} a & a+b \\ c & c+d \end{pmatrix}$ is used for the third edge. Thus to determine the contribution of the third edge we must consider $-d'/c' = -(c+d)/c = -1 - d/c$. Suppose first that $-d/c = \pm\infty$ and hence $-d'/c' = \pm\infty$. Using Table 1, we see that the three edges contribute $(0,0), (0,-2\beta)$ and $(0,0)$ respectively, for a sum of $(0,-2\beta)$. Next, suppose $-\infty < -d/c < 0$ and thus $-\infty < -d'/c' < 0$. Now the edges contribute $(\beta,\beta), (0,-2\beta)$ and $(-\beta,-\beta)$, giving the same total as before. As our next case, suppose $0 < -d/c < 1$ and hence $-\infty < -d'/c' < 0$. The edges now contribute $(-\beta,-\beta), (2\beta,0)$ and $(-\beta,-\beta)$, again

giving a sum of $(0,-2\beta)$. Finally, if $1 < -d/c < \infty$, then $0 < -d'/c' < \infty$ and we obtain $(-\beta,-\beta)+(0,-2\beta)+(\beta,\beta) = (0,-2\beta)$.

The computations for the other regions are similar and are left to the reader. □

Proof of Theorem 4.1. Let γ be a path in D_t with endpoints in D_1 and let γ' be obtained from γ by pushing each "diagonal" edge across a region of type R_0 through R_3 (as in Lemma 4.3) to eliminate all edges of type C and D. Thus $M(\gamma') = k(\alpha,\beta)$ for some integer k. Notice that any path in D_1 must pass through fractions whose denominators alternate in parity. Thus if γ' starts at $\frac{1}{0}$ and ends at $\frac{p}{q}$ it must have a number of edges equivalent to $q \mod 2$. Since the first edge contributes zero to k and every other edge contributes ± 1, we have that k and q have opposite parity.

To go back to γ from γ' suppose that we must move across n_0^+ regions of type R_0 (or R_2) in the positive sense and n_0^- in the negative sense. Similarly, let n_1^+ and n_1^- be the number of regions of type R_1 (or R_3) that we must push across in the positive or negative sense respectively. Then

$$\begin{aligned} M(\gamma) &= k(\alpha,\beta) + (n_0^+ - n_0^-)(0,-2\beta) + (n_1^+ - n_1^-)(-\alpha+\beta,\alpha-\beta) \\ &= ((k - n_1^+ + n_1^-)\alpha + (n_1^+ - n_1^-)\beta, \\ &\qquad (n_1^+ - n_1^-)\alpha + (k - n_1^+ + n_1^- - 2n_0^+ + 2n_0^-)\beta). \end{aligned}$$

Thus

$$\begin{aligned} x &= k - n_1^+ + n_1^-, \\ y &= n_1^+ - n_1^-, \\ z &= k - n_1^+ + n_1^- - 2n_0^+ + 2n_0^- \end{aligned}$$

and $x \equiv z \mod 2$. Furthermore, $x + y = k$. Thus if the path begins at $\frac{1}{0}$ and ends at $\frac{p}{q}$ we see that $x + y \equiv 1 + q \mod 2$. □

The following lemma, which is analogous to Lemma 4.3, allows us to handle the case where C-type edges are replaced with A-type edges in D_1. The proof is similar to the proof of Lemma 4.3 and is left to the reader.

Lemma 4.4. *Let* $g = \begin{pmatrix} a & b \\ c & d \end{pmatrix}$ *be any element of* G *where* b *is even and label the regions of* $g(Q)$ *as shown in Figure* 7. *If* $\gamma_i = \partial S_i$, *oriented counterclockwise, then*

$$\begin{aligned} M(\gamma_0) &= (-2\beta + 2n, -2n) \text{ and} \\ M(\gamma_1) &= (-2n, -2\beta + 2n) \end{aligned}$$

where $0 \le n \le \beta$.

Using this lemma we may determine the form of $M(\gamma)$ for any path in D_1.

Theorem 4.5. *Let* γ *be any path in* D_1. *Then* $M(\gamma)$ *has the form*

$$M(\gamma) = ((x + ys)\beta, (x - ys)\beta)$$

where y *is the number of* C*-type edges in* γ *and* s *is a rational parameter with* $-1 \le s \le 1$. *If additionally,* γ *begins at* $\frac{1}{0}$ *and ends at* $\frac{p}{q}$, *then* $x + y \equiv 1 + q \mod 2$.

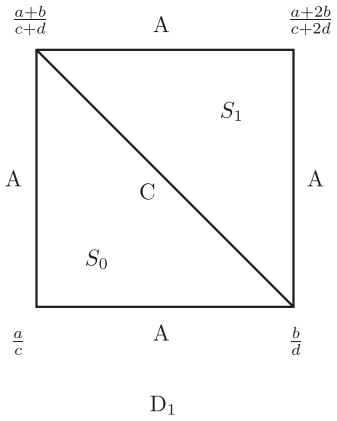

FIGURE 7. Lemma 4.4 describes the result of traveling around each region.

Proof. If γ has no C-type edges the result is the same as Lemma 4.2. If C-type edges are present, push each such edge across a region of type S_0 (as in Lemma 4.4) to obtain a path with only A-type edges. Applying Lemma 4.4, we now have that

$$M(\gamma) = k(\beta,\beta) + \sum_{i=1}^{P}(-2\beta + 2n_i, -2n_i) - \sum_{i=P+1}^{P+N}(-2\beta + 2n_i, -2n_i)$$

for some integer k, nonnegative integers P and N, and integers n_i where $0 \le n_i \le \beta$. Let

$$X = 2\sum_{i=1}^{P} n_i - 2\sum_{i=P+1}^{P+N} n_i.$$

If we let

$$s = \frac{X - (P-N)\beta}{(P+N)\beta},$$

then it is not hard to show that $-1 \le s \le 1$. Substituting for X in $M(\gamma)$ we obtain the desired result with $y = P + N$ and $x = k - P + N$. □

Theorems 4.1 and 4.5 place restrictions on the form of $M(\gamma)$ where γ is a path in either D_t or D_1. The following theorem shows that these are in fact the only restrictions that apply and moreover that minimal paths may be used to realize any desired value of $M(\gamma)$.

Theorem 4.6. *There exist minimal paths in either D_t or D_1 which begin at $\frac{1}{0}$ and end at some $\frac{p}{q}$ that realize all possible values of M subject only to the constraints of Theorems* 4.1 *and* 4.5.

Proof. Focussing on Theorem 4.1, let x, y, and z be any three integers such that $x \equiv z \mod 2$. Suppose also that $x + y \equiv 1 \mod 2$. We seek a fraction $\frac{p}{q}$, with q even, and a minimal path γ from $\frac{1}{0}$ to $\frac{p}{q}$ such that $M(\gamma) = (x\alpha + y\beta, y\alpha + z\beta)$. Referring to the proof of Theorem 4.1, we will show how to build a minimal path with compete control over k, n_0^+, n_0^-, n_1^+, and n_1^-.

Figure 8 shows six blocks of quadrilaterals, each containing a minimal path. Heavy dots are placed at vertices with even denominators. Starting with either of

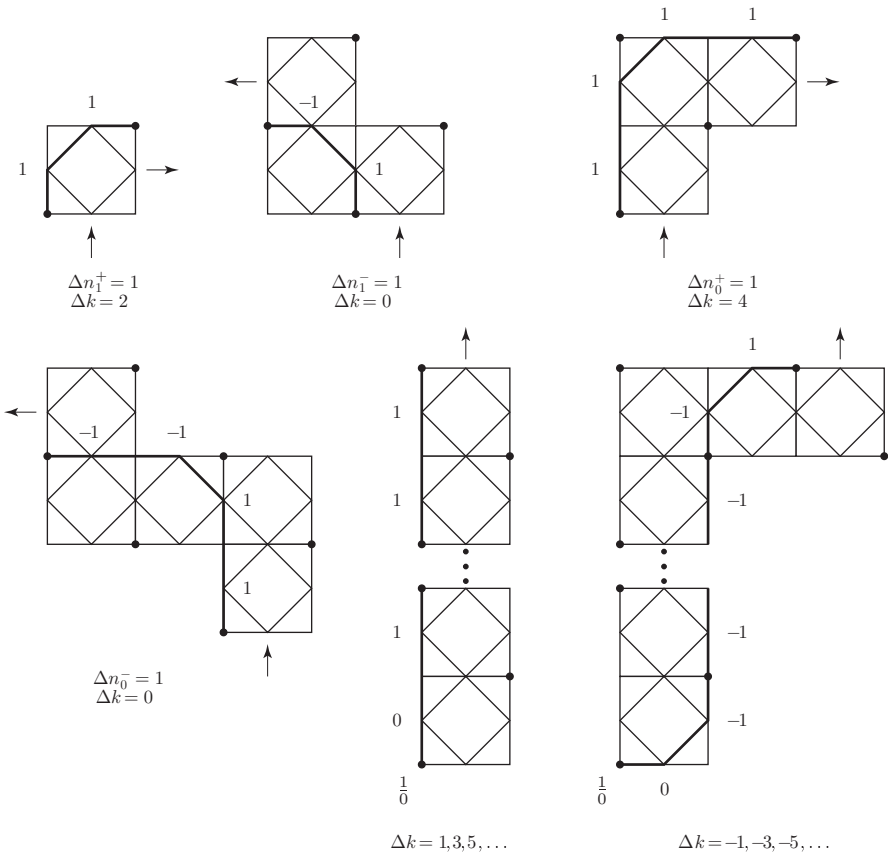

FIGURE 8. Building blocks for a minimal path γ with desired $M(\gamma)$.

the last two blocks in the second row, we may then paste on any number of the first four blocks (in any order), always gluing blocks together as indicated by the arrows. No matter how the blocks are joined together, the path will remain minimal. The first four blocks involve C and D type edges and can be used to create any desired values for n_0^+, n_0^-, n_1^+, and n_1^-. Once these parameters are fixed, a sufficiently long starting block of one of the two types may be prepended to create any desired value of k.

It is not hard to adapt this argument to the case where $x + y \equiv 0 \mod 2$ or to the case of Theorem 4.5. Moreover, more efficient sets of building blocks than these can easily be designed. □

5. An example

In this section we will apply our improved algorithm to compute the boundary slopes of the links $\mathcal{L}_{\frac{4k-1}{8k}}$. Since $\frac{4k-1}{8k}$ has the continued fraction expansion $[0, 2, -2k, -2]$, these links can be pictured as shown in Figure 9. Here we have replaced the $-2k$ right-handed crossings with $\frac{1}{k}$-surgery on an unknot surrounding

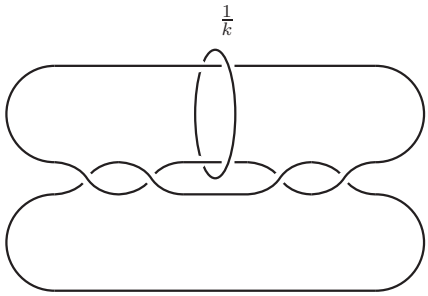

FIGURE 9. The links $\mathcal{L}_k$

the parallel strands. Viewed this way we see that $\mathcal{L}_{\frac{4k-1}{8k}}$, which we will henceforth simply denote as $\mathcal{L}_k$, is $\frac{1}{k}$ surgery on one component of the Borromean rings.

The minimal chain of quadrilaterals in the diagram D_t connecting $\frac{1}{0}$ to $\frac{4k-1}{8k}$ is abstractly depicted in Figure 10. It is not hard to show by induction that for $k > 1$ there are precisely six minimal paths, $\{\gamma_1, \ldots, \gamma_6\}$, in D_t from $\frac{1}{0}$ to $\frac{4k-1}{8k}$. These are listed in Table 2 by listing the consecutive vertices in each path. The vertices R_i, S_i, and T_i each lie between two vertices of D_1 (or D_0) as indicated in the figure. If $k = 1$, path γ_4 is no longer minimal and should be deleted from the list.

Associated to each of these paths, in the case where $t > 1$, is a weighted branched surface with $\alpha > \beta$. To find the boundary slopes of surfaces carried by such a branched surface we must first compute the intersection numbers (M_1, M_2) and then adjust for our choice of basis. We will derive (M_1, M_2) from each path by using the lemmas given in the last section.

Let σ_1 be the path in D_1 given by $\sigma_1 = \{\frac{1}{0}, \frac{1}{1}, \frac{1}{2}, \frac{2k}{4k+1}, \frac{4k-1}{8k}\}$. It follows easily from Lemma 4.2 that $M(\sigma_1) = (3\alpha, 3\beta)$. We may now deform σ_1 to γ_1 by moving the path over two regions, each of type R_1 (or R_3) as shown in Figure 6. This results in adding $2(-\alpha + \beta, \alpha - \beta)$. We therefore obtain $(2\alpha + \beta, \alpha + 2\beta)$. To pass to either γ_2 or γ_3, we deform γ_1 across two regions of type R_0 and one of type R_4.

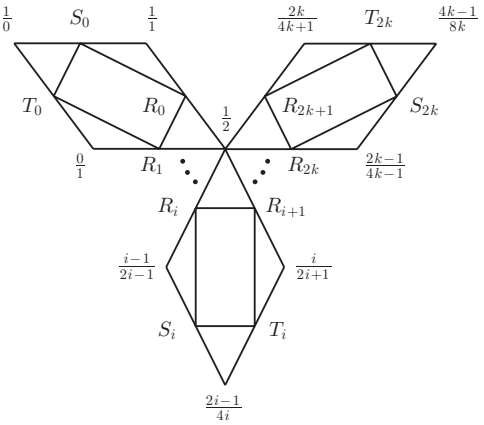

FIGURE 10. The minimal chain of quadrilaterals from $\frac{1}{0}$ to $\frac{4k-1}{8k}$.

TABLE 2. Minimal D_t paths from $\frac{1}{0}$ to $\frac{4k-1}{8k}$.

γ_1: $\frac{1}{0}, S_0, R_0, \frac{1}{2}, R_{2k+1}, T_{2k}, \frac{4k-1}{8k}$

γ_2: $\frac{1}{0}, S_0, R_0, \frac{1}{2}, R_{2k}, S_{2k}, \frac{4k-1}{8k}$

γ_3: $\frac{1}{0}, T_0, R_1, \frac{1}{2}, R_{2k+1}, T_{2k}, \frac{4k-1}{8k}$

γ_4: $\frac{1}{0}, T_0, R_1, \frac{1}{2}, R_{2k}, S_{2k}, \frac{4k-1}{8k}$

γ_5: $\frac{1}{0}, T_0, R_1, R_2, \ldots, R_{2k}, S_{2k}, \frac{4k-1}{8k}$

γ_6: $\frac{1}{0}, T_0, \frac{0}{1}, S_1, T_1, \frac{1}{3}, S_2, T_2, \ldots, \frac{2k-1}{4k-1}, S_{2k}, \frac{4k-1}{8k}$

In either case then, we must add $(-2\beta, -2\alpha)$ and obtain a total of (α, β). To move from γ_2 (or γ_3) to γ_4, we again move across two regions of type R_0 and one of type R_4 and again add $(-2\beta, -2\alpha)$. This gives $(\alpha - 2\beta, -2\alpha + \beta)$ for $M(\gamma_4)$. We may now obtain γ_5 from γ_4 by moving across $2k-1$ regions of type R_0. Thus the value of $M(\gamma_5)$ is $(\alpha - 2\beta, -2\alpha + \beta) + (2k-1)(0, -2\beta) = (\alpha - 2\beta, -2\alpha + (3-4k)\beta)$. Now let $\sigma_2 = \{\frac{1}{0}, \frac{0}{1}, \frac{1}{2}, \frac{2k-1}{4k-1}, \frac{4k-1}{8k}\}$. We may either think of moving γ_4 to σ_2, or start over again with Lemma 4.3. Either way we obtain $(-\alpha, -\beta)$ for $M(\sigma_2)$. Finally, to obtain γ_6 from σ_2, we must move across $2k-1$ regions, each made up of one region of type R_0, two of type R_1 and one of type R_4. This results in adding $(2k-1)(-2\alpha, 0)$ to $M(\sigma_2)$ giving a total of $((1-4k)\alpha, -\beta)$.

We have now accounted for all the possibilities when $\alpha > \beta$. We may determine all cases where $\beta = 0$, and thus $t = \infty$, from these by substitution, but letting α equal β does not give all possibilities for $t = 1$. Because both γ_5 and γ_6 involve C-type edges, so do their limiting minimal edge paths in D_1. In this example, both γ_5 and γ_6 limit to the same minimal edge path γ_5^1 in D_1. To recover all possible boundary slopes when $\alpha = \beta$ we must now consider the branched surface corresponding to this path where C-type surfaces are replaced with A-type surfaces.

Starting from σ_2 we may move to γ_5^1 by moving across k regions of type S_0 and $k-1$ regions of type S_1. Thus we must add $\sum_{i=1}^{k}(-2\beta + 2n_{2i-1}, -2n_{2i-1})$ and $\sum_{i=1}^{k-1}(-2n_{2i}, -2\beta + 2n_{2i})$ to $M(\sigma_2) = (-\alpha, -\beta)$. This gives $(-(1+2k)\beta + X, (1-2k)\beta - X)$, where $X = 2\sum_{i=1}^{2k-1}(-1)^{i+1}n_i$. Here $0 \le n_i \le \beta$.

The final 4-tuples $(M_1, \alpha, M_2, \beta)$ for $\mathcal{L}_{\frac{4k-1}{8k}}$ in all cases where $\alpha \ge \beta \ge 0$ are given in Table 3. All of these data are still with respect to the basis $\{\mu_i, \lambda_i\}$.

From Table 3 we may easily derive the corresponding 4-tuples when $0 \le \alpha \le \beta$. Namely, $(M_1(\alpha, \beta), \alpha, M_2(\alpha, \beta), \beta)$ is changed to $(M_2(\beta, \alpha), \alpha, M_1(\beta, \alpha), \beta)$. Notice that if a minimal path in D_t does not involve any C-type edges, then the contributions to M_1 and M_2 given in Table 1 are equal when $\alpha = \beta$. Thus the same 4-tuple will result as we approach $\frac{\alpha}{\beta} = 1$ from either above or below. Using Equation (3.1) it is not difficult to show that $\mathrm{lk}(\lambda_1, K_1) = \mathrm{lk}(\lambda_2, K_2) = -1$ for all k. The final boundary slopes M_1/α and M_2/β for all rational values of t, and with respect to the preferred basis are now given in Table 4. Furthermore, the slopes in this table are described by the rational parameters $t = \alpha/\beta$ in the case where $\alpha \ne \beta$, and

$$s = \frac{X - \beta}{(2k-1)\beta}$$

in the case where $\alpha = \beta$. Note that a pair of boundary slopes of the form $(0, \phi)$ means that the corresponding surface has no boundary components on K_2 (and a slope of zero on K_1).

TABLE 3. Boundary slope data for $\mathcal{L}_{\frac{4k-1}{8k}}$, $k > 0$, with respect to the basis $\{\mu_1, \lambda_1\}$ and for $\alpha \geq \beta$. The path γ_4 is not counted if $k = 1$. Here $X = n_1 - n_2 + n_3 - \cdots + n_{2k-1}$.

path	algebraic intersection with $(\lambda_1, \mu_1, \lambda_2, \mu_2)$	restrictions
γ_1	$(\alpha + 2\beta, \alpha, 2\alpha + \beta, \beta)$	$\alpha > \beta \geq 0$
γ_2	$(\alpha, \alpha, \beta, \beta)$	$\alpha > \beta \geq 0$
γ_3	$(\alpha, \alpha, \beta, \beta)$	$\alpha > \beta \geq 0$
γ_4	$(\alpha - 2\beta, \alpha, -2\alpha + \beta, \beta)$	$\alpha > \beta \geq 0$
γ_5	$(\alpha - 2\beta, \alpha, -2\alpha + (3-4k)\beta, \beta)$	$\alpha > \beta \geq 0$
γ_6	$((1-4k)\alpha, \alpha, -\beta, \beta)$	$\alpha > \beta \geq 0$
γ_5^1	$(-(1+2k)\beta + 2X, \beta, (1-2k)\beta - 2X, \beta)$	$0 \leq n_i \leq \beta = \alpha$

TABLE 4. Boundary slope pairs for $\mathcal{L}_{\frac{4k-1}{8k}}$, $k > 0$, with respect to the preferred basis $\{\mu_1, \lambda_1^0\}$. Both t and s are rational parameters.

∂-slopes	restrictions
$(0, 0)$	
$(0, \phi), (\phi, 0)$	
$(-4k, \phi), (\phi, -4k)$	
$(-4k, -2), (-2, -4k)$	
$(2t^{-1}, 2t)$	$0 \leq t \leq \infty$
$(-2t^{-1}, -2t)$	$0 \leq t \leq \infty, k > 1$
$(-2t^{-1} + 2 - 4k, -2t)$	$0 \leq t \leq 1$
$(-2t^{-1}, 2 - 4k - 2t)$	$1 \leq t \leq \infty$
$(-1 - 2k + (2k-1)s, -1 - 2k - (2k-1)s)$	$-1 \leq s \leq 1$

6. Boundary slopes of 2-bridge links up to 10 crossings

We have written a computer program to implement the algorithm described in Section 4. One begins by finding all minimal paths in D_0 and D_1 from $\frac{1}{0}$ to $\frac{p}{q}$. These determine the minimal paths in D_t. Each minimal path γ in D_t is then deformed into a path γ' of only A and B-type edges. Lemma 4.2 is used to compute $M(\gamma')$, and $M(\gamma)$ is derived from this using Lemma 4.3. In order to minimize the chance of producing errors, each of us coded a program independent of the other with debugging proceeding until our results agreed.

The second Tait conjecture states that any reduced alternating diagram of a link is minimal. Thus is it easy to determine the crossing number of $\mathcal{L}_{p/q}$. If we express p/q as the continued fraction $[0, a_2, \ldots, a_n]$ where each a_i is positive, then $\mathcal{L}_{p/q}$ has a reduced alternating 4-plat diagram with $a_2 + a_3 + \cdots + a_n$ crossings. Thus the crossing number of $\mathcal{L}_{p/q}$ is $a_2 + a_3 + \cdots + a_n$. It is now a simple matter to determine all 2-bridge links with 10 or fewer crossings by finding all such continued fractions. Furthermore, from the classification of 2-bridge links, we know precisely when two fractions represent the same link.

The boundary slopes of all 2-bridge links having ten or less crossings are presented in Tables 5-9. All slopes are with respect to a preferred longitude and meridian basis. For those links with 9 or less crossings, the index of the link in Rolfsen's

table [11] is also given. Two types of data are listed. First, all boundary slopes in the case where $1 < t < \infty$ are given. Note that the 4-tuple of intersection numbers corresponding to the entry $(f(t), g(t))$ is $(\alpha f(\alpha/\beta), \alpha, \beta g(\alpha/\beta), \beta)$. From these we obtain the algebraic intersection numbers $(\alpha g(\beta/\alpha), \alpha, \beta f(\beta/\alpha), \beta)$ for $0 < t < 1$ as described earlier. Thus, the boundary slopes for $0 < t < 1$ are $(g(t^{-1}), f(t^{-1}))$. Furthermore, one may then derive from these all boundary slopes in the cases $t = 0$ and $t = \infty$ and some of the boundary slopes in the case $t = 1$. Recall that if α or β equals zero, then there is a sign ambiguity in the first or third entry respectively of the associated 4-tuple. In addition, we have not sought to remove data that may correspond to meridionally compressible surfaces. Finally, all additional slopes in the case $t = 1$ are given in terms of the rational parameter s with $-1 \le s \le 1$. Here the pair $(f(s), g(s))$ corresponds to the 4-tuple $(\beta f(s), \beta, \beta g(s), \beta)$.

TABLE 5. Boundary slope data for 2-bridge links to 8 crossings. Parameters t and s are rational with $1 < t < \infty$ and $-1 \le s \le 1$.

link	p/q	boundary slopes			
2_1^2	1/2	$(-t^{-1}, -t)$	(t^{-1}, t)		
4_1^2	1/4	$(-2, -2)$	$(-2t^{-1}, -2t)$	$(2t^{-1}, 2t)$	
5_1^2	3/8	$(-4, -2)$	$(0, 0)$	$(-2t^{-1}, -2 - 2t)$	$(2t^{-1}, 2t)$
		$(-3 + s, -3 - s)$			
6_1^2	1/6	$(-3, -3)$	$(-3t^{-1}, -3t)$	$(3t^{-1}, 3t)$	
6_2^2	3/10	$(-2 - t^{-1}, -2 - t)$	$(2 - t^{-1}, -t)$	$(-2 + t^{-1}, t)$	$(2 + t^{-1}, 2 + t)$
		$(-3t^{-1}, -3t)$	$(3t^{-1}, 3t)$	$(s, -s)$	
6_3^2	5/12	$(-6, -2)$	$(0, 0)$	$(-2t^{-1}, -4 - 2t)$	$(-2t^{-1}, -2t)$
		$(2t^{-1}, 2t)$	$(-4 + 2s, -4 - 2s)$		
7_1^2	3/14	$(-5, -3)$	$(-2 - t^{-1}, -4 - t)$	$(-2 + t^{-1}, -2 + t)$	$(-3t^{-1}, -2 - 3t)$
		$(-t^{-1}, -t)$	(t^{-1}, t)	$(3t^{-1}, 3t)$	$(-4 + s, -4 - s)$
7_3^2	7/16	$(-8, -2)$	$(0, 0)$	$(-2t^{-1}, -6 - 2t)$	$(-2t^{-1}, -2t)$
		$(2t^{-1}, 2t)$	$(-5 + 3s, -5 - 3s)$		
7_2^2	5/18	$(-2 - t^{-1}, -2 - t)$	$(4 - t^{-1}, -t)$	$(-2 + t^{-1}, -2 + t)$	$(-2 + t^{-1}, 2 + t)$
		$(4 + t^{-1}, 2 + t)$	$(-3t^{-1}, -3t)$	$(-t^{-1}, -t)$	(t^{-1}, t)
		$(3t^{-1}, 2 + 3t)$	$(4 + s, 4 - s)$	$(1 + 2s, 1 - 2s)$	
8_1^2	1/8	$(-4, -4)$	$(-4t^{-1}, -4t)$	$(4t^{-1}, 4t)$	
8_2^2	3/16	$(0, -2)$	$(2 - 2t^{-1}, -2t)$	$(-3 - t^{-1}, -3 - t)$	$(-3 + t^{-1}, -1 + t)$
		$(2 + 2t^{-1}, 2 + 2t)$	$(-4t^{-1}, -4t)$	$(4t^{-1}, 4t)$	$(-1 + s, -1 - s)$
8_6^2	9/20	$(-10, -2)$	$(0, 0)$	$(-2t^{-1}, -8 - 2t)$	$(-2t^{-1}, -2t)$
		$(2t^{-1}, 2t)$	$(-6 + 4s, -6 - 4s)$		
8_3^2	5/22	$(-7, -3)$	$(-2 - t^{-1}, -6 - t)$	$(-2 - t^{-1}, -2 - t)$	$(-2 + t^{-1}, -2 + t)$
		$(-3t^{-1}, -4 - 3t)$	$(-3t^{-1}, -3t)$	$(-t^{-1}, -t)$	(t^{-1}, t)
		$(3t^{-1}, 3t)$	$(-5 + 2s, -5 - 2s)$		
8_4^2	7/24	$(-4, -4)$	$(-4, 0)$	$(2, 0)$	$(-2 - 2t^{-1}, -2 - 2t)$
		$(2 - 2t^{-1}, -2 - 2t)$	$(-2 + 2t^{-1}, 2t)$	$(2 + 2t^{-1}, 2 + 2t)$	$(-4t^{-1}, -4t)$
		$(4t^{-1}, 4t)$	$(1 + s, 1 - s)$	$(-2 + 2s, -2 - 2s)$	
8_5^2	7/26	$(-2 - t^{-1}, -2 - t)$	$(6 - t^{-1}, -t)$	$(-2 + t^{-1}, -2 + t)$	$(-2 + t^{-1}, 4 + t)$
		$(6 + t^{-1}, 2 + t)$	$(-3t^{-1}, -3t)$	$(-t^{-1}, -t)$	(t^{-1}, t)
		$(3t^{-1}, 3t)$	$(3t^{-1}, 4 + 3t)$	$(5 + 2s, 5 - 2s)$	$(2 + 3s, 2 - 3s)$
8_7^2	11/30	$(-7, -3)$	$(-4 - t^{-1}, -4 - t)$	$(-4 + t^{-1}, -2 + t)$	$(-3t^{-1}, -4 - 3t)$
		$(-t^{-1}, -2 - t)$	$(-t^{-1}, -t)$	(t^{-1}, t)	$(3t^{-1}, 3t)$
		$(-2 + s, -2 - s)$	$(-5 + 2s, -5 - 2s)$		
8_8^2	13/34	$(-4 - t^{-1}, -2 - t)$	$(4 - t^{-1}, -2 - t)$	$(4 - t^{-1}, 2 - t)$	$(-4 + t^{-1}, -2 + t)$
		$(-4 + t^{-1}, 2 + t)$	$(4 + t^{-1}, 2 + t)$	$(-3t^{-1}, -2 - 3t)$	$(-t^{-1}, -2 - t)$
		$(-t^{-1}, -t)$	(t^{-1}, t)	$(t^{-1}, 2 + t)$	$(3t^{-1}, 2 + 3t)$
		$(-4 + s, -4 - s)$	$(-2 + s, -2 - s)$	$(3s, -3s)$	$(2 + s, 2 - s)$
		$(4 + s, 4 - s)$			

TABLE 6. Boundary slope data for 2-bridge links with 9 crossings. Parameters t and s are rational with $1 < t < \infty$ and $-1 \le s \le 1$.

link	p/q	boundary slopes			
9_1^2	3/20	$(-6,-4)$	$(-3-t^{-1},-5-t)$	$(-3+t^{-1},-3+t)$	$(-4t^{-1},-2-4t)$
		$(-2t^{-1},-2t)$	$(2t^{-1},2t)$	$(4t^{-1},4t)$	$(-5+s,-5-s)$
9_4^2	5/24	$(-6,-4)$	$(-4,-6)$	$(0,0)$	$(-2-2t^{-1},-4-2t)$
		$(-2+2t^{-1},-2+2t)$	$(-4t^{-1},-2-4t)$	$(4t^{-1},4t)$	$(-5+s,-5-s)$
9_{10}^2	11/24	$(-12,-2)$	$(0,0)$	$(-2t^{-1},-10-2t)$	$(-2t^{-1},-2t)$
		$(2t^{-1},2t)$	$(-7+5s,-7-5s)$		
9_2^2	5/28	$(2,-2)$	$(4-2t^{-1},-2t)$	$(-3-t^{-1},-3-t)$	$(-3+t^{-1},-3+t)$
		$(-3+t^{-1},1+t)$	$(4+2t^{-1},2+2t)$	$(-4t^{-1},-4t)$	$(-2t^{-1},-2t)$
		$(2t^{-1},2t)$	$(4t^{-1},2+4t)$	$(2s,-2s)$	$(5+s,5-s)$
9_3^2	7/30	$(-9,-3)$	$(-2-t^{-1},-8-t)$	$(-2-t^{-1},-2-t)$	$(-2+t^{-1},-2+t)$
		$(-3t^{-1},-6-3t)$	$(-3t^{-1},-3t)$	$(-t^{-1},-t)$	(t^{-1},t)
		$(3t^{-1},3t)$	$(-6+3s,-6-3s)$		
9_5^2	7/32	$(0,-4)$	$(0,0)$	$(-2-2t^{-1},-4-2t)$	$(2-2t^{-1},-2-2t)$
		$(2-2t^{-1},2-2t)$	$(-5-t^{-1},-3-t)$	$(-5+t^{-1},-1+t)$	$(-2+2t^{-1},-2+2t)$
		$(2+2t^{-1},2+2t)$	$(-4t^{-1},-2-4t)$	$(4t^{-1},4t)$	$(-5+s,-5-s)$
		$(-2+2s,-2-2s)$			
9_8^2	9/34	$(-2-t^{-1},-2-t)$	$(8-t^{-1},-t)$	$(-2+t^{-1},-2+t)$	$(-2+t^{-1},6+t)$
		$(8+t^{-1},2+t)$	$(-3t^{-1},-3t)$	$(-t^{-1},-t)$	(t^{-1},t)
		$(3t^{-1},3t)$	$(3t^{-1},6+3t)$	$(6+3s,6-3s)$	$(3+4s,3-4s)$
9_6^2	11/36	$(-2,-2)$	$(-2,0)$	$(2,2)$	$(-2-2t^{-1},-2-2t)$
		$(2-2t^{-1},-2t)$	$(5-t^{-1},1-t)$	$(5+t^{-1},3+t)$	$(-2+2t^{-1},2+2t)$
		$(2+2t^{-1},4+2t)$	$(-4t^{-1},-4t)$	$(-2t^{-1},-2t)$	$(2t^{-1},2t)$
		$(4t^{-1},2+4t)$	$(-1+s,-1-s)$	$(5+s,5-s)$	$(2+2s,2-2s)$
9_9^2	11/40	$(-4,-4)$	$(-4,2)$	$(0,0)$	$(4,0)$
		$(-2-2t^{-1},-2-2t)$	$(4-2t^{-1},-2-2t)$	$(-2+2t^{-1},-2+2t)$	$(-2+2t^{-1},2+2t)$
		$(4+2t^{-1},2+2t)$	$(-4t^{-1},-4t)$	$(4t^{-1},2+4t)$	$(5+s,5-s)$
		$(2+2s,2-2s)$	$(-1+3s,-1-3s)$		
9_7^2	13/44	$(-6,-4)$	$(-6,0)$	$(-2,-2)$	$(-2,0)$
		$(2,-2)$	$(2,0)$	$(2,2)$	$(-4-2t^{-1},-2-2t)$
		$(-2-2t^{-1},-4-2t)$	$(2-2t^{-1},-4-2t)$	$(2-2t^{-1},-2t)$	$(-4+2t^{-1},2t)$
		$(-2+2t^{-1},2t)$	$(2+2t^{-1},2+2t)$	$(-4t^{-1},-2-4t)$	$(-2t^{-1},-2t)$
		$(2t^{-1},2t)$	$(4t^{-1},4t)$	$(-5+s,-5-s)$	$(-1+s,-1-s)$
		$(2s,-2s)$	$(1+s,1-s)$	$(-3+3s,-3-3s)$	
9_{11}^2	17/46	$(-9,-3)$	$(-6-t^{-1},-4-t)$	$(-4-t^{-1},-6-t)$	$(-4-t^{-1},-2-t)$
		$(-6+t^{-1},-2+t)$	$(-4+t^{-1},-2+t)$	$(-3t^{-1},-6-3t)$	$(-3t^{-1},-2-3t)$
		$(-t^{-1},-4-t)$	$(-t^{-1},-2-t)$	$(-t^{-1},-t)$	(t^{-1},t)
		$(3t^{-1},3t)$	$(-4+s,-4-s)$	$(-2+s,-2-s)$	$(-3+2s,-3-2s)$
		$(-6+3s,-6-3s)$			
9_{12}^2	19/50	$(-4-t^{-1},-2-t)$	$(6-t^{-1},-2-t)$	$(6-t^{-1},2-t)$	$(-4+t^{-1},-2+t)$
		$(-4+t^{-1},4+t)$	$(6+t^{-1},2+t)$	$(-3t^{-1},-2-3t)$	$(-t^{-1},-2-t)$
		$(-t^{-1},-t)$	(t^{-1},t)	$(t^{-1},4+t)$	$(3t^{-1},3t)$
		$(3t^{-1},4+3t)$	$(-4+s,-4-s)$	$(-2+s,-2-s)$	$(3+2s,3-2s)$
		$(5+2s,5-2s)$	$(1+4s,1-4s)$		

TABLE 7. Boundary slope data for 2-bridge links with 10 crossings (part 1). Parameters t and s are rational with $1 < t < \infty$ and $-1 \le s \le 1$.

p/q	boundary slopes			
1/10	$(-5,-5)$	$(-5t^{-1},-5t)$	$(5t^{-1},5t)$	
3/22	$(-1,-3)$	$(2-3t^{-1},-3t)$	$(-4-t^{-1},-4-t)$	$(-4+t^{-1},-2+t)$
	$(2+3t^{-1},2+3t)$	$(-5t^{-1},-5t)$	$(5t^{-1},5t)$	$(-2+s,-2-s)$
5/26	$(-1,1)$	$(1,-1)$	$(-3-2t^{-1},-3-2t)$	$(3-2t^{-1},1-2t)$
	$(-3+2t^{-1},-1+2t)$	$(3+2t^{-1},3+2t)$	$(-5t^{-1},-5t)$	$(5t^{-1},5t)$
	$(s,-s)$			
13/28	$(-14,-2)$	$(0,0)$	$(-2t^{-1},-12-2t)$	$(-2t^{-1},-2t)$
	$(2t^{-1},2t)$	$(-8+6s,-8-6s)$		
5/32	$(-8,-4)$	$(-3-t^{-1},-7-t)$	$(-3-t^{-1},-3-t)$	$(-3+t^{-1},-3+t)$
	$(-4t^{-1},-4-4t)$	$(-4t^{-1},-4t)$	$(-2t^{-1},-2t)$	$(2t^{-1},2t)$
	$(4t^{-1},4t)$	$(-6+2s,-6-2s)$		
7/38	$(-5,-5)$	$(-5,-1)$	$(-2-3t^{-1},-2-3t)$	$(2-3t^{-1},-2-3t)$
	$(-3-2t^{-1},-3-2t)$	$(2-t^{-1},-t)$	$(2+t^{-1},t)$	$(-3+2t^{-1},-1+2t)$
	$(-2+3t^{-1},3t)$	$(2+3t^{-1},2+3t)$	$(-5t^{-1},-5t)$	$(-t^{-1},-4-t)$
	$(t^{-1},-2+t)$	$(5t^{-1},5t)$	$(s,-s)$	$(2+s,2-s)$
	$(-3+2s,-3-2s)$			
9/38	$(-11,-3)$	$(-2-t^{-1},-10-t)$	$(-2-t^{-1},-2-t)$	$(-2+t^{-1},-2+t)$
	$(-3t^{-1},-8-3t)$	$(-3t^{-1},-3t)$	$(-t^{-1},-t)$	(t^{-1},t)
	$(3t^{-1},3t)$	$(-7+4s,-7-4s)$		
7/40	$(4,-2)$	$(6-2t^{-1},-2t)$	$(-3-t^{-1},-3-t)$	$(-3+t^{-1},-3+t)$
	$(-3+t^{-1},3+t)$	$(6+2t^{-1},2+2t)$	$(-4t^{-1},-4t)$	$(-2t^{-1},-2t)$
	$(2t^{-1},2t)$	$(4t^{-1},4t)$	$(4t^{-1},4+4t)$	$(6+2s,6-2s)$
	$(1+3s,1-3s)$			
9/40	$(-8,-4)$	$(-4,-8)$	$(-4,-4)$	$(0,0)$
	$(-2-2t^{-1},-6-2t)$	$(-2-2t^{-1},-2-2t)$	$(-2+2t^{-1},-2+2t)$	$(-4t^{-1},-4-4t)$
	$(-4t^{-1},-4t)$	$(4t^{-1},4t)$	$(-6+2s,-6-2s)$	
11/42	$(-2-t^{-1},-2-t)$	$(10-t^{-1},-t)$	$(-2+t^{-1},-2+t)$	$(-2+t^{-1},8+t)$
	$(10+t^{-1},2+t)$	$(-3t^{-1},-3t)$	$(-t^{-1},-t)$	(t^{-1},t)
	$(3t^{-1},3t)$	$(3t^{-1},8+3t)$	$(7+4s,7-4s)$	$(4+5s,4-5s)$
13/42	$(3,1)$	$(-2-3t^{-1},-2-3t)$	$(3-2t^{-1},-1-2t)$	$(-4-t^{-1},-4-t)$
	$(-4+t^{-1},t)$	$(3+2t^{-1},3+2t)$	$(-2+3t^{-1},3t)$	$(-5t^{-1},-5t)$
	$(-t^{-1},-t)$	$(t^{-1},2+t)$	$(5t^{-1},5t)$	$(2+s,2-s)$
	$(-1+2s,-1-2s)$			
11/48	$(0,-6)$	$(0,0)$	$(-2-2t^{-1},-6-2t)$	$(-2-2t^{-1},-2-2t)$
	$(2-2t^{-1},-4-2t)$	$(2-2t^{-1},2-2t)$	$(-7-t^{-1},-3-t)$	$(-7+t^{-1},-1+t)$
	$(-2+2t^{-1},-2+2t)$	$(2+2t^{-1},2+2t)$	$(-4t^{-1},-4-4t)$	$(-4t^{-1},-4t)$
	$(4t^{-1},4t)$	$(-6+2s,-6-2s)$	$(-3+3s,-3-3s)$	
17/48	$(-8,-4)$	$(-2,-4)$	$(0,0)$	$(-2-2t^{-1},-6-2t)$
	$(-5-t^{-1},-5-t)$	$(-5+t^{-1},-3+t)$	$(-2+2t^{-1},-2+2t)$	$(-4t^{-1},-4-4t)$
	$(-2t^{-1},-2-2t)$	$(2t^{-1},2t)$	$(4t^{-1},4t)$	$(-3+s,-3-s)$
	$(-6+2s,-6-2s)$			

TABLE 8. Boundary slope data for 2-bridge links with 10 crossings (part 2). Parameters t and s are rational with $1 < t < \infty$ and $-1 \le s \le 1$.

p/q	boundary slopes			
11/52	$(-8,-4)$	$(-6,-6)$	$(-2,-4)$	$(-2,-2)$
	$(0,-2)$	$(0,0)$	$(-4-2t^{-1},-4-2t)$	$(-2-2t^{-1},-6-2t)$
	$(-5-t^{-1},-5-t)$	$(-5+t^{-1},-3+t)$	$(-4+2t^{-1},-2+2t)$	$(-2+2t^{-1},-2+2t)$
	$(-4t^{-1},-4-4t)$	$(-2t^{-1},-2-2t)$	$(-2t^{-1},-2t)$	$(2t^{-1},2t)$
	$(4t^{-1},4t)$	$(-3+s,-3-s)$	$(-1+s,-1-s)$	$(-6+2s,-6-2s)$
15/56	$(-4,-4)$	$(-4,4)$	$(0,0)$	$(6,0)$
	$(-2-2t^{-1},-2-2t)$	$(6-2t^{-1},-2-2t)$	$(-2+2t^{-1},-2+2t)$	$(-2+2t^{-1},4+2t)$
	$(6+2t^{-1},2+2t)$	$(-4t^{-1},-4t)$	$(4t^{-1},4t)$	$(4t^{-1},4+4t)$
	$(4s,-4s)$	$(6+2s,6-2s)$	$(3+3s,3-3s)$	
17/56	$(-2,-2)$	$(-2,0)$	$(2,0)$	$(2,2)$
	$(2,4)$	$(4,2)$	$(-2-2t^{-1},-2-2t)$	$(2-2t^{-1},-2t)$
	$(7-t^{-1},1-t)$	$(7+t^{-1},3+t)$	$(-2+2t^{-1},2t)$	$(-2+2t^{-1},4+2t)$
	$(2+2t^{-1},2+2t)$	$(2+2t^{-1},6+2t)$	$(-4t^{-1},-4t)$	$(-2t^{-1},-2t)$
	$(2t^{-1},2t)$	$(4t^{-1},4t)$	$(4t^{-1},4+4t)$	$(-1+s,-1-s)$
	$(1+s,1-s)$	$(6+2s,6-2s)$	$(3+3s,3-3s)$	
17/58	$(-2-3t^{-1},-2-3t)$	$(2-3t^{-1},-2-3t)$	$(2-3t^{-1},-3t)$	$(-4-t^{-1},-4-t)$
	$(-4-t^{-1},-t)$	$(-2-t^{-1},-t)$	$(2-t^{-1},-t)$	$(4-t^{-1},-2-t)$
	$(4-t^{-1},2-t)$	$(-4+t^{-1},-2+t)$	$(-4+t^{-1},2+t)$	$(-2+t^{-1},t)$
	$(2+t^{-1},t)$	$(4+t^{-1},t)$	$(4+t^{-1},4+t)$	$(-2+3t^{-1},3t)$
	$(-2+3t^{-1},2+3t)$	$(2+3t^{-1},2+3t)$	$(-5t^{-1},-5t)$	$(-t^{-1},-2-t)$
	$(t^{-1},2+t)$	$(5t^{-1},5t)$	$(-2+s,-2-s)$	$(s,-s)$
	$(3s,-3s)$	$(2+s,2-s)$	$(-3+2s,-3-2s)$	$(3+2s,3-2s)$
13/60	$(-2,-4)$	$(-2,-2)$	$(0,0)$	$(0,2)$
	$(2,-4)$	$(2,0)$	$(-2-2t^{-1},-4-2t)$	$(4-2t^{-1},-2-2t)$
	$(4-2t^{-1},2-2t)$	$(-5-t^{-1},-3-t)$	$(-5+t^{-1},-3+t)$	$(-5+t^{-1},1+t)$
	$(-2+2t^{-1},2t)$	$(4+2t^{-1},2+2t)$	$(-4t^{-1},-2-4t)$	$(-2t^{-1},-2-2t)$
	$(-2t^{-1},-2t)$	$(2t^{-1},2t)$	$(4t^{-1},2+4t)$	$(-5+s,-5-s)$
	$(-3+s,-3-s)$	$(1+s,1-s)$	$(5+s,5-s)$	$(-1+3s,-1-3s)$
23/62	$(-11,-3)$	$(-8-t^{-1},-4-t)$	$(-4-t^{-1},-8-t)$	$(-4-t^{-1},-2-t)$
	$(-8+t^{-1},-2+t)$	$(-4+t^{-1},-2+t)$	$(-3t^{-1},-8-3t)$	$(-3t^{-1},-2-3t)$
	$(-t^{-1},-6-t)$	$(-t^{-1},-2-t)$	$(-t^{-1},-t)$	(t^{-1},t)
	$(3t^{-1},3t)$	$(-4+s,-4-s)$	$(-2+s,-2-s)$	$(-4+3s,-4-3s)$
	$(-7+4s,-7-4s)$			
19/64	$(-8,-4)$	$(-8,0)$	$(-2,-2)$	$(-2,0)$
	$(2,-4)$	$(2,0)$	$(2,2)$	$(-6-2t^{-1},-2-2t)$
	$(-2-2t^{-1},-6-2t)$	$(-2-2t^{-1},-2-2t)$	$(2-2t^{-1},-6-2t)$	$(2-2t^{-1},-2t)$
	$(-6+2t^{-1},2t)$	$(-2+2t^{-1},2t)$	$(2+2t^{-1},2+2t)$	$(-4t^{-1},-4-4t)$
	$(-4t^{-1},-4t)$	$(-2t^{-1},-2t)$	$(2t^{-1},2t)$	$(4t^{-1},4t)$
	$(-1+s,-1-s)$	$(1+s,1-s)$	$(-6+2s,-6-2s)$	$(-1+3s,-1-3s)$
	$(-4+4s,-4-4s)$			

TABLE 9. Boundary slope data for 2-bridge links with 10 crossings (part 3). The parameters t and s are rational with $1 < t < \infty$ and $-1 \le s \le 1$.

p/q	boundary slopes			
23/64	$(-2,-4)$	$(-2,-2)$	$(-2,0)$	$(0,-2)$
	$(0,0)$	$(4,0)$	$(4,2)$	$(-2-2t^{-1},-4-2t)$
	$(4-2t^{-1},-2-2t)$	$(-5-t^{-1},-3-t)$	$(-5+t^{-1},-3+t)$	$(-5+t^{-1},1+t)$
	$(-2+2t^{-1},-2+2t)$	$(-2+2t^{-1},2+2t)$	$(4+2t^{-1},2+2t)$	$(-4t^{-1},-2-4t)$
	$(-2t^{-1},-2-2t)$	$(-2t^{-1},-2t)$	$(2t^{-1},2t)$	$(2t^{-1},2+2t)$
	$(4t^{-1},2+4t)$	$(-5+s,-5-s)$	$(-3+s,-3-s)$	$(3+s,3-s)$
	$(5+s,5-s)$	$(2+2s,2-2s)$	$(-1+3s,-1-3s)$	
25/66	$(-4-t^{-1},-2-t)$	$(8-t^{-1},-2-t)$	$(8-t^{-1},2-t)$	$(-4+t^{-1},-2+t)$
	$(-4+t^{-1},6+t)$	$(8+t^{-1},2+t)$	$(-3t^{-1},-2-3t)$	$(-t^{-1},-2-t)$
	$(-t^{-1},-t)$	(t^{-1},t)	$(t^{-1},6+t)$	$(3t^{-1},3t)$
	$(3t^{-1},6+3t)$	$(-4+s,-4-s)$	$(-2+s,-2-s)$	$(4+3s,4-3s)$
	$(6+3s,6-3s)$	$(2+5s,2-5s)$		
19/68	$(-2,-2)$	$(-2,2)$	$(0,0)$	$(0,2)$
	$(2,0)$	$(2,4)$	$(4,2)$	$(-2-2t^{-1},-2-2t)$
	$(4-2t^{-1},2-2t)$	$(4-2t^{-1},-2t)$	$(7-t^{-1},1-t)$	$(7+t^{-1},3+t)$
	$(-2+2t^{-1},2t)$	$(-2+2t^{-1},4+2t)$	$(4+2t^{-1},4+2t)$	$(-4t^{-1},-4t)$
	$(-2t^{-1},-2t)$	$(2t^{-1},2t)$	$(2t^{-1},2+2t)$	$(4t^{-1},4+4t)$
	$(2s,-2s)$	$(1+s,1-s)$	$(3+s,3-s)$	$(6+2s,6-2s)$
	$(3+3s,3-3s)$			
29/70	$(-11,-3)$	$(-6-t^{-1},-6-t)$	$(-6-t^{-1},-2-t)$	$(-6+t^{-1},-2+t)$
	$(-3t^{-1},-8-3t)$	$(-3t^{-1},-4-3t)$	$(-3t^{-1},-3t)$	$(-t^{-1},-4-t)$
	$(-t^{-1},-t)$	(t^{-1},t)	$(3t^{-1},3t)$	$(-5+2s,-5-2s)$
	$(-3+2s,-3-2s)$	$(-7+4s,-7-4s)$		
31/74	$(-6-t^{-1},-2-t)$	$(6-t^{-1},-4-t)$	$(6-t^{-1},2-t)$	$(-6+t^{-1},-2+t)$
	$(-6+t^{-1},4+t)$	$(6+t^{-1},2+t)$	$(-3t^{-1},-4-3t)$	$(-3t^{-1},-3t)$
	$(-t^{-1},-4-t)$	$(-t^{-1},-t)$	(t^{-1},t)	$(t^{-1},4+t)$
	$(3t^{-1},3t)$	$(3t^{-1},4+3t)$	$(5s,-5s)$	$(-5+2s,-5-2s)$
	$(-3+2s,-3-2s)$	$(3+2s,3-2s)$	$(5+2s,5-2s)$	
21/76	$(-6,-4)$	$(-6,2)$	$(-2,-2)$	$(-2,2)$
	$(0,-2)$	$(0,0)$	$(4,-2)$	$(4,0)$
	$(4,2)$	$(-4-2t^{-1},-2-2t)$	$(-2-2t^{-1},-4-2t)$	$(4-2t^{-1},-4-2t)$
	$(4-2t^{-1},-2t)$	$(-4+2t^{-1},-2+2t)$	$(-4+2t^{-1},2+2t)$	$(-2+2t^{-1},-2+2t)$
	$(-2+2t^{-1},2+2t)$	$(4+2t^{-1},2+2t)$	$(-4t^{-1},-2-4t)$	$(-2t^{-1},-2t)$
	$(2t^{-1},2t)$	$(2t^{-1},2+2t)$	$(4t^{-1},2+4t)$	$(-5+s,-5-s)$
	$(-1+s,-1-s)$	$(2s,-2s)$	$(3+s,3-s)$	$(5+s,5-s)$
	$(2+2s,2-2s)$	$(1+3s,1-3s)$	$(-2+4s,-2-4s)$	
31/80	$(-8,-4)$	$(-8,0)$	$(-4,-2)$	$(-4,0)$
	$(0,0)$	$(2,-2)$	$(2,2)$	$(-4-2t^{-1},-4-2t)$
	$(2-2t^{-1},-6-2t)$	$(2-2t^{-1},-2-2t)$	$(2-2t^{-1},2-2t)$	$(-4+2t^{-1},2t)$
	$(2+2t^{-1},2+2t)$	$(-4t^{-1},-4-4t)$	$(-2t^{-1},-2-2t)$	$(2t^{-1},2t)$
	$(4t^{-1},4t)$	$(-3+s,-3-s)$	$(2s,-2s)$	$(-6+2s,-6-2s)$
	$(-2+2s,-2-2s)$	$(-4+4s,-4-4s)$		

References

1. Gerhard Burde and Heiner Zieschang. *Knots*, volume 5 of *de Gruyter Studies in Mathematics*. Walter de Gruyter & Co., Berlin, 2003. MR1959408 (2003m:57005)
2. M. Culler and P. Shalen. Varieties of group representations and splittings of 3-manifolds. *Annals of Mathematics*, 117:109–146, 1983. MR683804 (84k:57005)
3. Nathan M. Dunfield. A table of boundary slopes of Montesinos knots. *Topology*, 40:309–315, 2001, arXiv:math.GT/9901120. MR1808223 (2001j:57008)
4. W. Floyd and A. Hatcher. The space of incompressible surfaces in a 2-bridge link complement. *Trans. Amer. Math. Soc.*, 305(2):575–599, 1988. MR924770 (89c:57004)
5. Ronald L. Graham, Donald E. Knuth, and Oren Patashnik. *Concrete mathematics*. Addison-Wesley Publishing Company, Reading, MA, 1994. MR1397498 (97d:68003)
6. A. Hatcher and U. Oertel. Boundary slopes for Montesinos knots. *Topology*, 28(4):453–480, 1989. MR1030987 (91e:57016)
7. A. Hatcher and W. Thurston. Incompressible surfaces in 2-bridge knot complements. *Invent. Math.*, 79(2):225–246, 1985. MR778125 (86g:57003)
8. Jim Hoste and Morwen Thistlethwaite. Knotscape. `http://www.math.utk.edu/~ morwen`, 1998.
9. Alan E. Lash. *Boundary curve space of the Whitehead link complement*. Ph.D. thesis, University of California, Santa Barbara, 1993.
10. Tomotada Ohtsuki. Ideal points and incompressible surfaces in two-bridge knot complements. *J. Math. Soc. Japan*, 46(1):51–87, 1994. MR1248091 (94k:57016)
11. Dale Rolfsen. *Knots and links*, volume 7 of *Mathematics Lecture Series*. Publish or Perish Inc., Houston, TX, 1990. MR1277811 (95c:57018)

Pitzer College, 1050 N. Mills Ave., Claremont, California 91711
E-mail address: `jhoste@pitzer.edu`

Loyola Marymount University, 1 LMU Dr., Los Angeles, California 90045-2659
E-mail address: `pshanahan@lmu.edu`